Available online at www.sciencedirect.com

SCIENCE DIRECT

Cement and Concrete Research 35 (2005) 2183 – 2191

Cement and Concrete Research

Electrical responses of carbon fiber reinforced cementitious composites to monotonic and cyclic loading

Bing Chen[a,*], Juanyu Liu[b], Keru Wu[c]

[a]Department of Civil Engineering, Shanghai Jiaotong University, Shanghai, 200240, PR China
[b]Department of Civil Engineering, Texas A & M University, College Station, TX 77843, USA
[c]State Key Laboratory of Concrete Materials Research, Tongji University, Shanghai, 200092 China

Received 6 April 2004; accepted 25 February 2005

Abstract

In this paper, the electrical responses of carbon fiber reinforced cementitious composites (CFRCC) to both monotonic and cyclic loading were investigated by electrical resistance measurements. Damage occurring within specimens was also investigated by acoustic emission (AE). Results indicated that the conductivity of the composite was related to the stress level. Under monotonic loading, the electrical resistance decreased with increasing stress at low stress levels and increased with increasing stress at higher stress levels. Under cyclic loading, at lower loading amplitude, the electrical resistance of the system showed reversibility with the change of the load, however, when the loading amplitude was larger, it showed the irreversible increase. Both cases indicated that the breakdown and rebuild-up process of the conductive network under pressure may be responsible for the stress dependency of conductivity. The damage occurring inside material can be monitored in real time by measuring the change in electrical resistance during loading and unloading.

Keywords: Carbon fiber reinforced cementitious composites (CFRCC); Electrical resistance; Compression; Positive/negative pressure coefficient effect of resistance

1. Introduction

Damage occurs when concrete structure is subjected to dynamic loading and continual monitoring of a structure is valuable for damage assessment and mitigation. The sensing of damage is conventionally performed by attached or embedded sensors, such as optical fibers or acoustic sensors. However, these sensors add to the cost, are in low durability, and in addition, the sensing volume and spatial resolution are limited. A new method of detecting damage by electrical resistance has been proposed [1–4], which is based on the notion that damage causes irreversible change in electrical resistance, while elastic strain causes reversible changes in electrical resistance.

CFRCC consisting of insulating cement matrix and conducting carbon fiber are well known [5–9] to show a large variation in electrical resistance with changes of composition and microstructure, and a large decrease in electrical resistance occurring through formation of conducting paths. In CFRCC containing electrical conduction paths, damage can be monitored by measuring the change of electrical resistance generated by microdeformation or change of connectivity of the conduction path under an external load [10–13].

This paper reports the electrical responses of CFRCC to monotonic and cyclic loading at different loading levels. The compressive stress–strain behavior and the overall resistance change were monitored simultaneously. The damage occurring within specimens was also detected by acoustic emission (AE). Based on the results, the possibility

* Corresponding author. Tel.: +86 21 54744255.
E-mail address: hntchen@sjtu.edu.cn (B. Chen).

0008-8846/$ - see front matter © 2005 Elsevier Ltd. All rights reserved.
doi:10.1016/j.cemconres.2005.02.004

Table 1
Properties of carbon fiber

Diameter (μm)	Density (g/cm^3)	Tensile strength (GPa)	Young's modules (GPa)	Elongation at break (%)	Carbon content (w_c%)	Electrical resistivity (Ω·cm)
7±0.2	1.78	>3.0	220∼240	1.25∼1.60	>95	$10^{-2}\sim10^{-3}$

of predicting fracture and detecting damage in CFRCC was assessed.

2. Experimental details

2.1. Materials and specimens

The carbon fibers were isotropic pitch-based and unsized. The fiber properties are shown in Table 1. Type III Portland cement was used and silica fume was used in the amount 15% of the cement mass. The sand used met ISO standard. The water-binder ratio was 0.45 and sand-binder ratio was 1.0.

The mortar mixtures were prepared in a laboratory mortar mixer, and the procedure was as follows:

1) 30% of total water was added to the mixer.
2) Carboxy-methylcellulose was added while stirring and then left for approximately 20 min to allow it to dissolve completely.
3) Carbon fibers were added to the water and stirred gently.
4) The remaining water was added into the mixer followed by the high-range water-reducing admixture. Silica fume was then added.
5) After the mixer ran for approximately 10 s at slow speed, cement was added and mixed for approximate 30 s.
6) Sand was added into the running mixer and the mixture was mixed for another 30 s.
7) The mixer ran at medium speed for approximate 1 min.

Cubic specimens, 70.7 mm × 70.7 mm × 70.7 mm were cast in plexiglass molds and six specimens were used for each test. Two copper electrodes, 70.7 mm × 80.0 mm × 0.2 mm, were embedded in the fresh mix. The distance between the copper electrodes is 62.0 mm. After 24 h, the specimens were removed from the molds and transferred to a moist-curing room for 27 days.

Generally, there are two types of electrical conduction in moist specimens: electronic and electrolytic. The former is through the motion of free electrons in the conductive phases, e.g. carbon fibers, and the latter is through the motion of ions in the pore solution. In this investigation, the principal contribution to the electrical conduction is expected to be electronic. Hence, one day prior to testing, the specimens were taken out and dried at 80 °C for 24 h to reduce the water in the samples, as required by the electrical resistance measurement [14].

2.2. Testing equipment

Electrical resistance was measured using a four-terminal technique using a Keithley model 220 as current source and a Keithley mode 619 for voltage and current measurements. Conductive silver paint was applied between sample surface and current electrode to ensure a better electrical contact between them. The current and voltage electrodes were 4 mm apart in the sample and the current electrodes were insulated from the machine clamp. The device was interfaced to a computer to record and process data. The minimum time required to obtain a measurement was 0.1 s. The compression tests were performed using an Instron 8501 Digital Servo hydraulic testing system, with a strain rate of 0.015 mm/min. A SPARTAN-AT 2000 AE system was used for AE data acquisition; the emitted AE signals during testing were detected by a sensor with a resonant frequency of 150 kHz. The AE signals were amplified with a 40-dB gain in a preamplifier and a 20-dB gain in the system. The threshold was set at 40 dB to eliminate a high signal/noise ratio [15]. A schematic diagram of the loading equipment and the electrical resistance measurement is shown in Fig. 1.

3. Test results and discussion

Good consistency was found for six specimens in the same set during the tests. Therefore, the test results presented here are all average values.

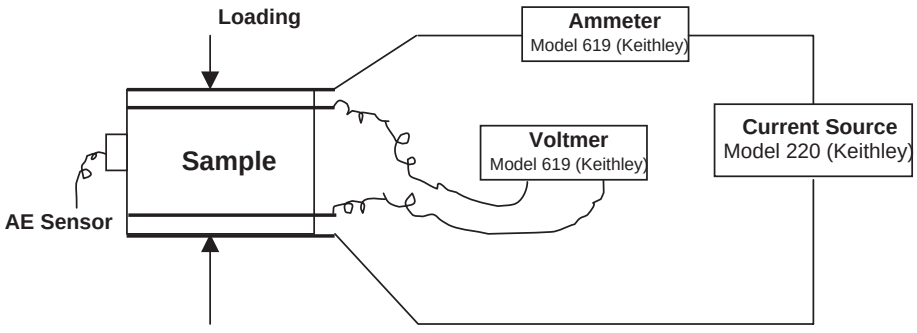

Fig. 1. Schematics of DC electrical measurement.

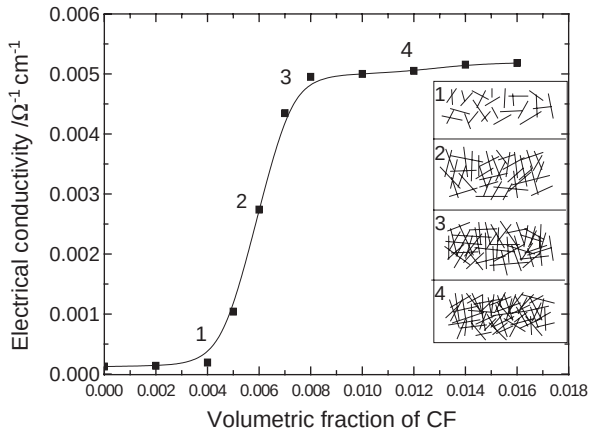

Fig. 2. Relationship between electrical conductivity and connectivity of conductivity carbon fibers.

3.1. Percolation network structure of carbon fiber in CFRCC

Fig. 2 shows the change of electrical conductivity at different carbon fiber contents. It can be seen that the electrical conductivity values of the composites increased with increasing carbon fiber volume fraction. The typical features of percolation phenomena have been described as follows.

(1) Before the volume fraction of carbon fiber reaches its threshold value of percolation (here, 0.5% of volume fraction), the conductivity increases by one or two orders of magnitude with the increase of carbon fiber content.

(2) After the volume fraction of carbon fiber reached its threshold value of percolation, the conductivity remains unchanged with the increase of carbon fiber content.

Fig. 3, SEM micrographs for carbon fibers distributed in the cement matrix, suggests that the change of conductivity with fiber content related to the connectivity change of fiber distributed in the cement matrix. At very low fiber content, carbon fiber was distributed homogeneously in the non-conductive matrix. There was minimal contact between adjacent fibers. As the carbon fiber content increases, fibers begin to connect with each other and it results in individual conduction clusters, and consequent increase of system conductivity. When the volume fraction of carbon fiber reaches its threshold value for percolation, the connected conductive network, formed due to contacts of carbon fibers within cement matrix, results in a more rapid increase in the conductivity. After the percolation threshold, the change of conductivity is not significant with the increase of carbon fiber content [14–16].

3.2. NPC and PPC effect in CFRCC under monotonic uniaxial compression

Fig.4 (a) illustrates the relation between applied stress level and fractional change in resistance (which refers to $(R-R_0)/R_0$) under monotonic uniaxial compression. It was

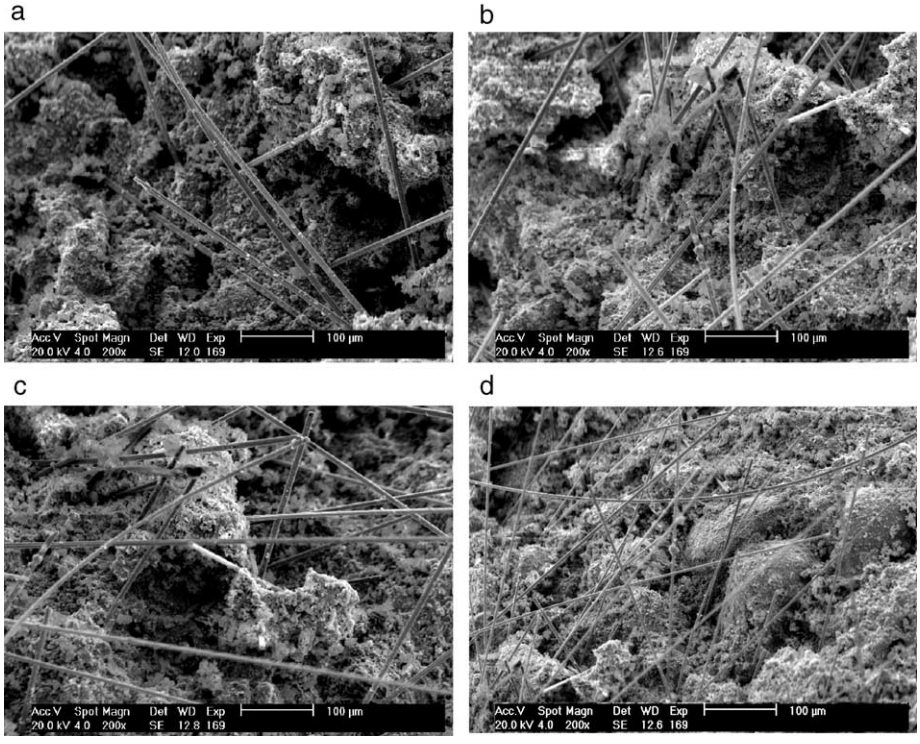

Fig. 3. SEM fractographs of CFRC with different carbon fibre volume (a) ϕ_f=0.002; (b) ϕ_f=0.004; (c) ϕ_f=0.0055; (d) ϕ_f=0.008.

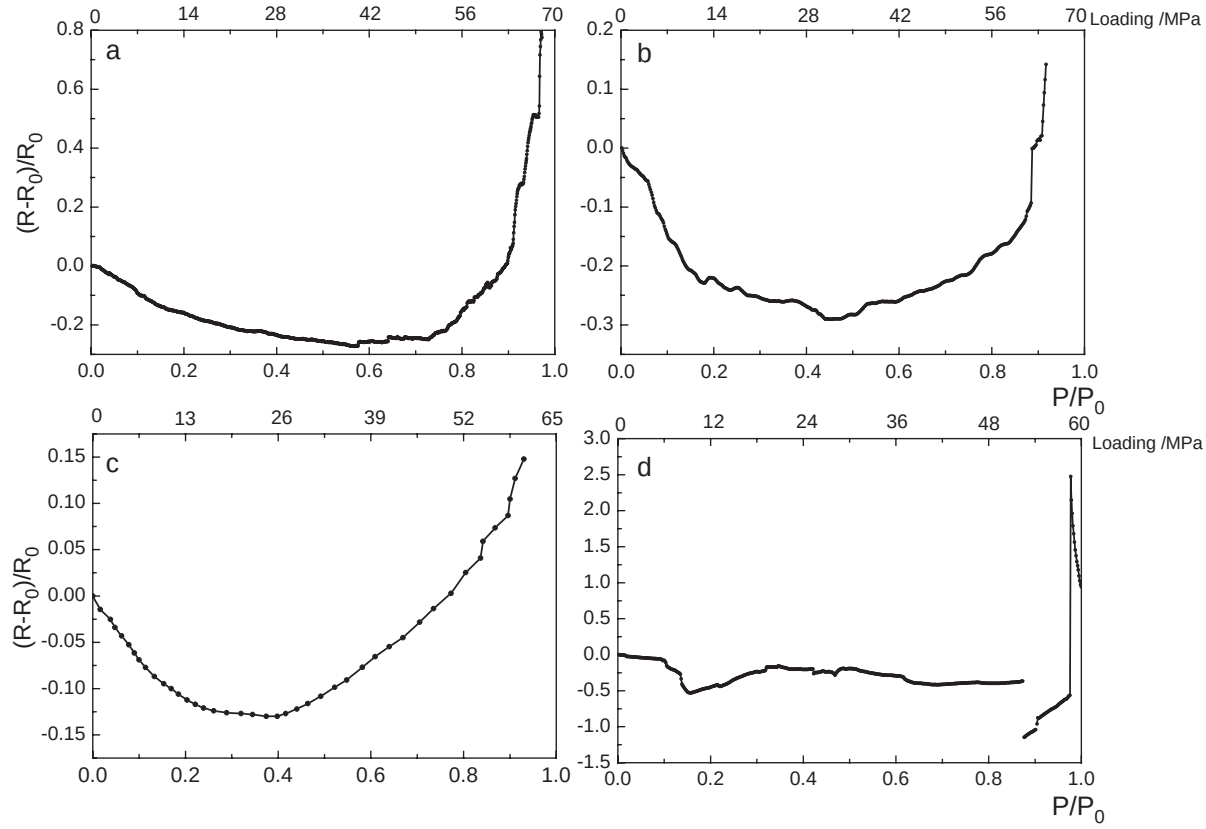

Fig. 4. Relationship between $\Delta R/R_0$ and P/P_{max} for CFRC at different carbon fiber content, (a) ϕ_f=0.008; (b) ϕ_f=0.0055; (c) ϕ_f=0.002; (d) ϕ_f=0.

observed that at a low stress level, the fractional change in resistance decreased with increasing stress level (named negative pressure coefficient effect, NPC effect). When the stress reached 57% of the fracture stress, a plateau appeared, where the fractional change in resistance remained almost constant. Shortly after that, the resistance increased rapidly with increasing stress (named positive pressure coefficient effect, PPC effect).

There are two interactive processes in CFRCC under exterior loading [17]:

(1) On the one hand, the compressive stress increases the chance for adjacent carbon fibers to connect with each other or decreases the gap between fibers. At the same time, those carbon fibers oriented along loading position will form a new conductive pathway. As a result, the system conductivity increases, i.e. fractional change of resistance decreases.
(2) On the other hand, cracking inside the specimen will occur due to loading, which will cause breakage of the existing conductive network. It results in a decrease in the system conductivity or an increase in the fractional change of resistance.

The breakdown and formation of the new percolation network under stresses is a dynamic balance process. The former is predominant during the initial loading stage, which is responsible for the formation of new networks, and consequently the decrease of resistivity with increasing stress. The counter-balancing of these two occurs when the stress reaches its critical value, which indicates some flaws occurring in the specimen. However, beyond the critical value, the latter becomes predominant and causes the existing network breakdown, which responds to PPC effect of resistance.

Fig. 4 presents the piezoresistance characteristics of system of CFRCC at different carbon fiber contents under monotonic uniaxial compression. It can be seen that there existed significant but different NPC and PPC effects of resistance in the system at different carbon fiber volume fractions. As shown in Table 2, the critical value of stress level, at which NPC effect switched to PPC effect, increased with increasing carbon fiber content. The sensitivity (the value of fraction change in resistance) of system to the load

Table 2
Stress level for minimum $\Delta R/R$ occurs and the smart behavior

Properties	Carbon fiber volume		
	0.20	0.55	0.80
Stress level at which the lowest $\Delta R/R$ occurs (%)	40	45	78
Lowest $\Delta R/R$	−0.128	−0.290	−0.260
$\Delta R/R$ at CFRCC failure	0.146	0.192	0.796

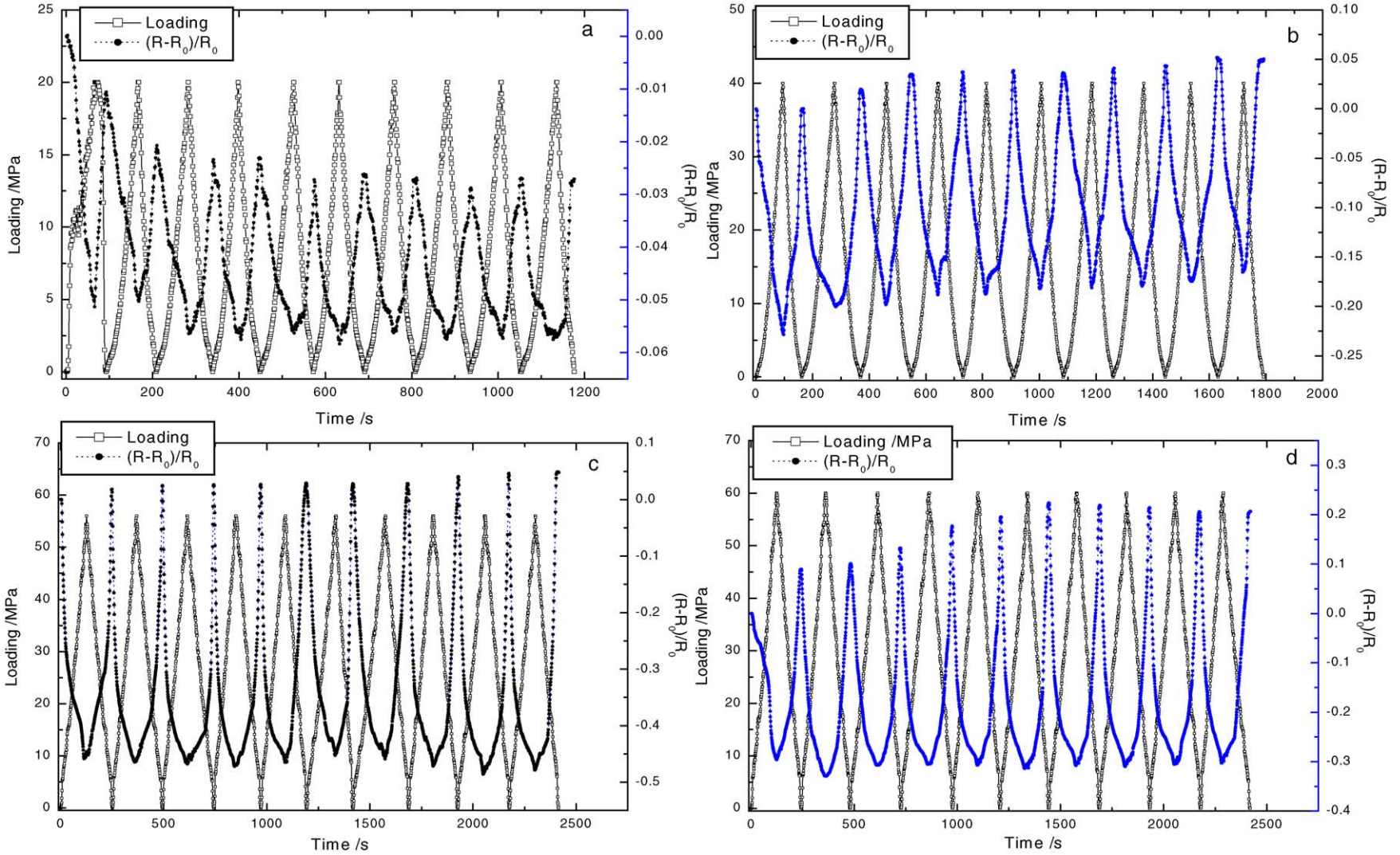

Fig. 5. Plots of $\Delta R/R_0$ vs. time and load vs. time during ten cycles of cyclic load for specimens at different stress amplitude (a) 30% of the fracture stress, (b) 60% of the fracture stress, (c) 80% of the fracture stress, (d) 90% of the fracture stress.

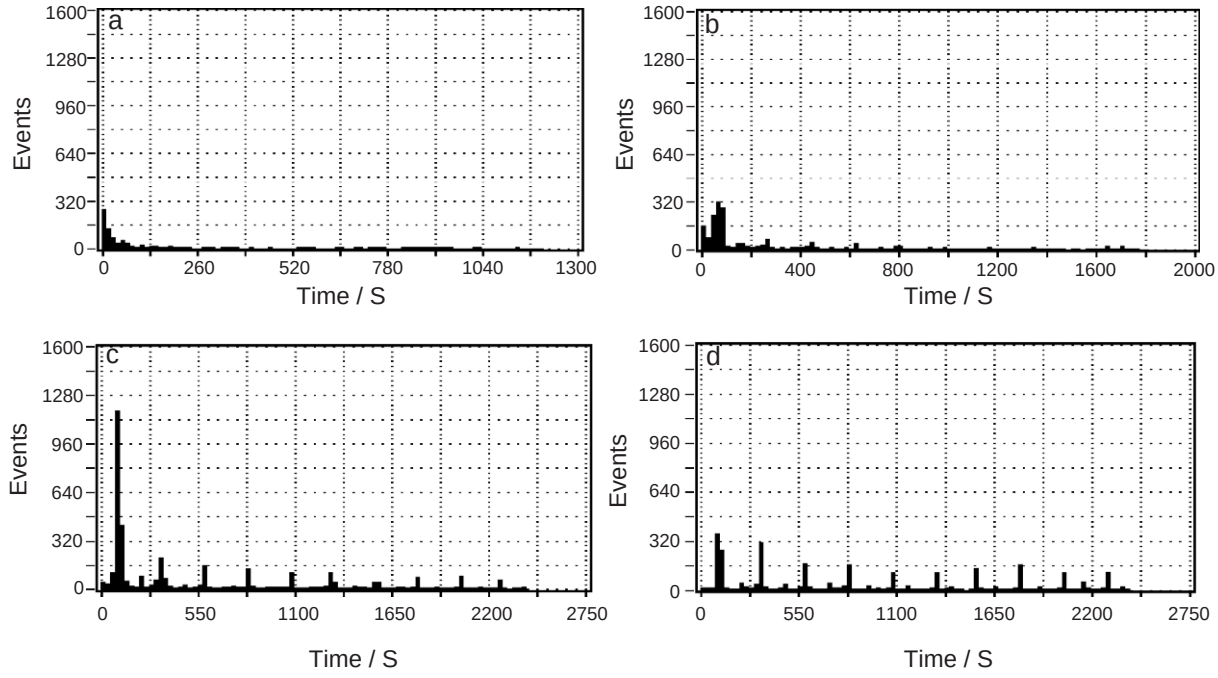

Fig. 6. Plots of events vs. time during ten cycles of cyclic load for specimens at different stress amplitude of (a) 30% of the fracture stress, (b) 60% of the fracture stress, (c) 80% of the fracture stress, (d) 90% of the fracture stress.

increased with increasing fiber volume fraction during failure. For the system without carbon fiber, piezoresistivity did not exist.

3.3. NPC and PPC effect in CFRCC under uniaxial cyclic compression

The characteristics of electrical responses for CFRCC (0.8% of fiber content) under cyclic compression at different stress amplitudes are shown in Fig. 5. There was a corresponding relation between fractional change in resistance and stress, i.e. in each cycle, the resistance decreased with loading, and linearly increased during unloading. However, there were some differences for different stress amplitudes. At low stress amplitude (shown in Fig. 5 (a), the stress amplitude was 30% of the compressive strength), there existed NPC effect upon loading in the first cycle. However, after the first cycle, there appeared an irreversible decrease (which refers to the fractional change in resistance do not return to zero in resistance after unloading which reduced gradually as load cycling progressed. After the fourth cycle, the changes in resistance became reversible, although it did not return to its initial value. In Fig. 5 (b) and (c), however, the fractional change in resistance returned to the initial value at the end of the first cycle. As the load cycling progressed, the resistance increased gradually after unloading cycle by cycle. In addition, PPC effects occurred during loading after 7 cycles in Fig. 5 (c). At a high stress amplitude (shown in Fig. 5 (d), the stress amplitude was 90% of the compressive strength), the PPC effect appeared during the first cycle and the fractional change in resistance returned to the initial value at the end of cycle. As load cycling progressed, $\Delta R/R_0$ increased more and more positively at zero load.

There also existed the breakdown and formation of the new percolation network during cyclic compressive loading. The rebuild process of the conductive network was predominant at low stress amplitude. The original flaws and pores in the specimen were compressed and possibly eliminated after the first two cycles during loading. Therefore, an irreversible deformation and then an irreversible decrease in resistance occurred. However, due to lower stress, no new cracks were forming during the subsequent loading and unloading cycles. The fractional change in resistance was thus reversible. When the stress amplitude was 60% of compressive strength, the re-build and breakdown processes of the conductive network kept counter

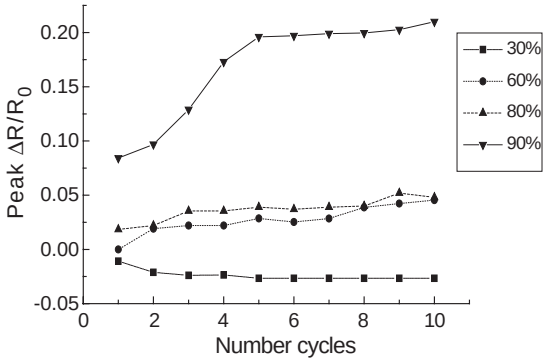

Fig. 7. Variation of the peak $\Delta R/R_0$ with cycle numbers at different stress amplitude of fracture stress for specimens.

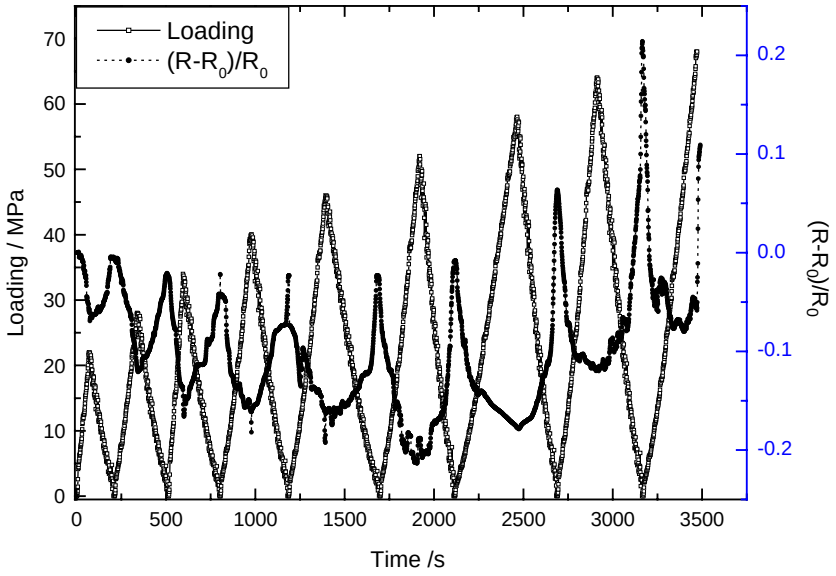

Fig. 8. Plots of $\Delta R/R_0$ vs. time and load vs. time during cycles of cyclic load with change stress.

balancing during the first several cycles. As load cycling progressed, the internal damage of the specimen increased and the breakdown process of the conductive network played predominant roles. The resistance could not return to its initial value after unloading and increases step by step due to the damage. When the stress amplitude reached 80%–90% of compressive strength, the continual damage occurring from the first cycle kept the breakdown process predominant. So, the fractional change in resistance did not return to zero at the end of each cycle, but increased cycle by cycle.

In order to verify the reliability of resistance measurement, AE measurement was used simultaneously during repetitive loading. Fig. 6 shows the corresponding relation between time and AE events during the repetitive loading at different stress amplitudes. In Fig. 6 (a) and (b), AE events only appeared during the first two loading cycles when the specimen was compacted. While during the subsequent loading cycles, there were almost no AE events and the fractional change in resistance was reversible. In Fig. 6 (c), and (d), different intensive AE events occurred in each loading cycle, which indicated corresponding internal damage. The peak in $\Delta R/R_0$, which reflects the damage in materials [18,19] as shown in Fig. 7, increased with progressive load cycles at high stress amplitude.

Fig. 8 shows the corresponding fractional change in resistance at an increase of 30 KN of load amplitude for each loading cycle. At low stress amplitude, there was a NPC effect, i.e. the resistance decreased upon loading and increased upon unloading in the first several cycles. However, when the stress amplitude reached 60% of compressive strength, an inverse change in resistance (PPC effect) occurred, i.e. $\Delta R/R_0$ gradually increased at the end of cycle. Fig. 9 shows the lowest and peak values of $\Delta R/R_0$ (at the end of each cycle) for all loading cycles. For comparison, Fig. 10 gives the plots of AE events for all cycles. During the first several cycles, some AE events

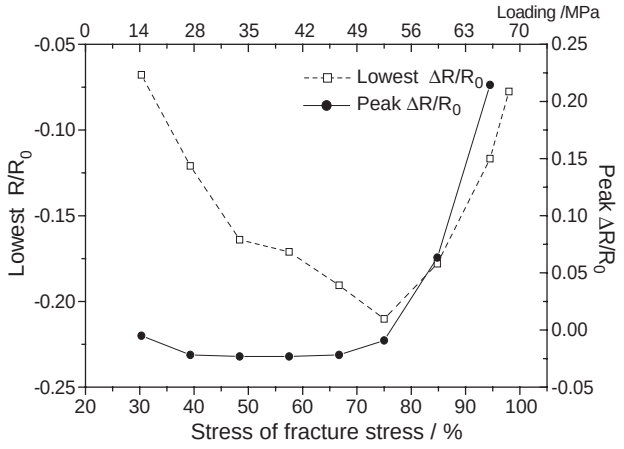

Fig. 9. Variation of the peak and lowest $\Delta R/R_0$ at different stress for specimens.

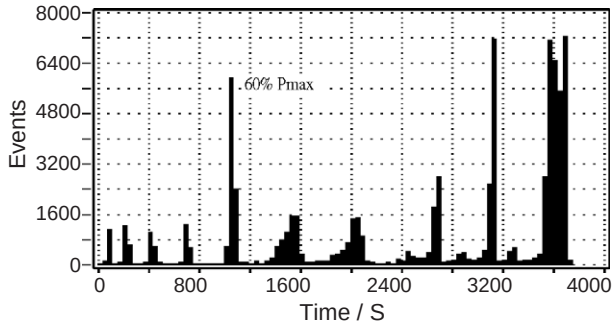

Fig. 10. Plots of events vs. time for specimen at cycle load with change stress.

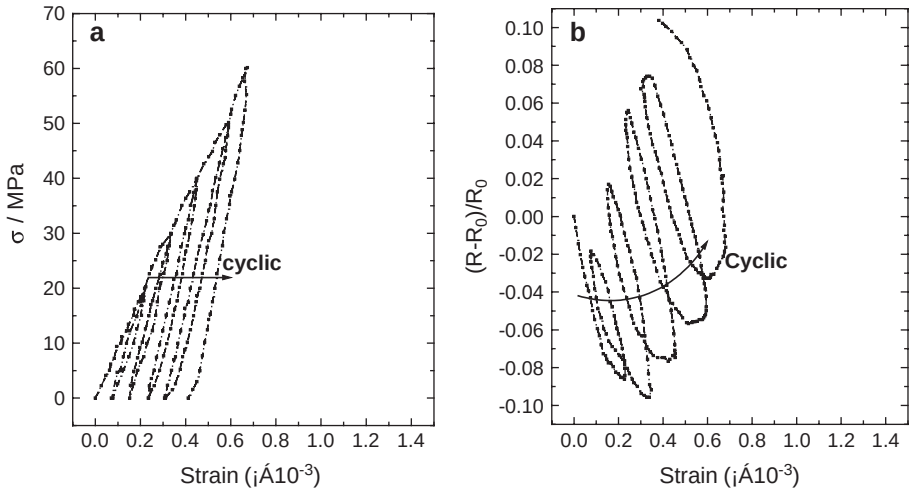

Fig. 11. Stress–strain–resistance relationship for CFRC (ϕ=0.008) subsequent to uniaxial compression cycles with maximum pressures increased step by step.

occurred and the resistance decreased irreversibly. This was mainly due to specimen compression and formation of new conductive pathways. As the stress amplitude reached 60% of compressive strength, AE events became intensive, which indicated there was significant internal damage and the conductive percolation network broke. At the same time, the peak and lowest values of $\Delta R/R_0$ increased significantly.

Fig. 11 shows the stress–strain–resistance curves of the system during repetitive compressive loading at increasing stress amplitude. In the first cycle, the fractional change in resistance decreased during loading and increased during unloading. However, the strain and fractional change in resistance did not return to zero after unloading and the value of fractional resistance was lower than zero. As load cycling progressed, the baseline of the resistance increased irreversibly and gradually cycle by cycle. The fractional resistance at zero load increased gradually cycle by cycle and the value was higher than zero.

There was a good correlation between the fractional change in resistance vs. the residual strain of specimen and the stress level vs. the residual strain of specimen, as shown in Fig. 11. During the first cycle of compression, the specimen was compressed and some pores and flaws inside the specimen were eliminated, and permanent strain occurred inside the material. As a result, the fractional resistance after decompression was irreversible and its value was negative. During subsequent loading cycles, the reversible part of $\Delta R/R_0$ was mainly due to dimensional changes, and corresponding reversible strain, while the irreversible part was due to damage. The great sensitivity of the irreversible part of $\Delta R/R_0$ to damage was also reflected by the significant non-zero value of the irreversible part of $\Delta R/R_0$ after merely the first cycle. Fig. 12

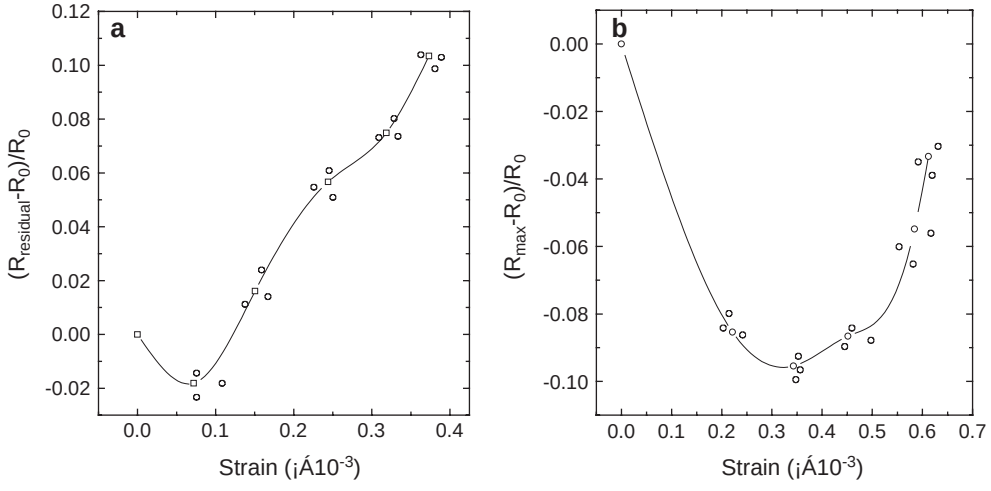

Fig. 12. Fractional changes in $R_{residual}$ and R_{max} as a function of strain for the CFRC (ϕ_f=0.8).

shows the fractional changes in maximum electrical resistance during loading $((R_{max}-R_0)/R_0)$ and residual resistance $((R_{residual}-R_0)/R_0)$, with the strain for the system. $R_{residual}$ is the associated resistance when the load gets back to zero, and R_{max} is the associated resistance when the pressure reaches the maximum value during every cyclic process. These relative changes in electrical resistance increased parabolically with the strain and were dependent on the maximum strain applied in the specimen. The observation from Figs. 11 and 12 showed that CFRCC were able to memorize strain applied in the system as the irreversible changes in $(R-R_0)/R_0$ (named Kaiser memory effect of resistance to residual deformation), which is useful for estimating the maximum strain applying to the composites.

4. Conclusions

(1) Short carbon fibers introduced to cement matrix homogeneously can increase the conductivity of system greatly. The conductivity of CFRCC can be described by percolation theory. In our research, when fiber content was 0.5% in volume, a continuous conductive network formed.
(2) There is a marked pressure dependence of the electrical resistance in CFRCC under both monotonic and cyclic compression. NPC and PPC effects of resistance exist under different stress levels. The breakdown and formation of the conductive network under pressure may be responsible for the pressure dependence of the conductivity.
(3) There exists Kaiser memory effect of resistance to residual deformation under repetitive loading. The results of AE monitoring in real time showed that the peak of $\Delta R/R_0$ increasing with loading cycles reflects the damage occurring inside material.
(4) With known initial resistance of the specimen, the loading and strain change history can be monitored by measuring fractional change of resistance. Therefore, monitoring the change in electrical resistance during loading and unloading by self-diagnosis of CFRCC was found to be a good method for detecting damage and fractures in material.

Acknowledgement

This work was supported by the University Key Studies Projects of Shanghai.

References

[1] P.W. Chen, D.D.L. Chung, Carbon fiber reinforced concrete as an intrinsically smart concrete for damage assessment during dynamic loading, Journal of Ceramics Society 78 (3) (1995) 816–818.
[2] X. Fu, D.D.L. Chung, Self-monitoring of fatigue damage in carbon reinforced cement, Cement and Concrete Research 26 (1) (1996) 15–20.
[3] Sugita Minoru, Yanagida Hiroakl, Materials design for self-diagnosis of fracture in CFGRP composite reinforcement, Smart Materials and Structures 4 (1A) (1995) A52–A57.
[4] D.D.L. Chung, Strain sensors based on the electrical resistance change accompanying the reversible pull-out of conducting short fibers in a less conducting matrix, Smart Materials and Structures 4 (1) (1995) 59–61.
[5] D.D.L. Chung, Cement-matrix composites for smart structures, Smart Materials and Structures 9 (4) (2000) 389–401.
[6] Z.Q. Shi, D.D.L. Chung, Concrete for magnetic shielding, Cement and Concrete Research 25 (5) (1995) 939–944.
[7] D.D.L. Chung, Cement reinforced with short carbon fibers: a multi-functional material, Composites. Part B, Engineering 31 (6–7) (2000) 511–526.
[8] K. Schulte, C. Baron, Load and failure analyses of CFRP laminates by means of electrical resistivity measurements, Composites Science and Technology 36 (1989) 63–76.
[9] Mohamed Boulfiza, Nemkumar Banthia, Application of continuum damage mechanics to carbon fiber-reinforced cement composites, ACI Materials Journal 97 (3) (2000) 245–253.
[10] Sihai Wei, D.D.L. Chung, Uniaxial compression in carbon fiber-reinforced cement, sensed by electrical resistivity measurement in longitudinal and transverse directions, Cement and Concrete Research 31 (2001) 297–301.
[11] Sihai Wei, D.D.L. Chung, Carbon fiber-reinforced cement as a strain-sensing coating, Cement and Concrete Research 31 (2001) 665–667.
[12] P.W. Chen, D.D.L. Chung, Concrete as a new strain/stress sensor, Composites. Part B, Engineering 27 (1) (1996) 10–23.
[13] D.D.L. Chung, Self-monitoring structural materials, Materials Science and Engineering R22 (1998) 57–58.
[14] Ping Xie, Ping Gu, R.J. Beaudoin, Electrical percolation phenomena in cement composites containing conductive fibres, Journal of Materials Science 31 (1996) 4093–4097.
[15] Keru Wu, Bing Chen, Wu Yao, Study of the influence of aggregate size distribution on mechanical properties of concrete by acoustic emission technique, Cement and Concrete Research 31 (2001) 919–923.
[16] P.K. Pramanik, D. Khastagir, T.N. Saha, Effect of extensional strain on the resistivity of electrically conductive nitrile-rubber composites filled with carbon fiber, Journal of Materials Science 28 (1993) 3539–3546.
[17] Bing Chen, Keru Wu, Wu Yao, Conductivity of carbon fiber reinforced cement-based composites, Cement and Concrete Composites 26 (2004) 291–297.
[18] Xiaojun Wang, Shoukai Wang, D.D.L. Chung, Sensing damage in carbon fiber and its polymer-matrix and carbon-matrix composites by electrical resistance measurement, Journal of Materials Science 34 (1999) 2703–2713.
[19] Dragos-Marian Bontea, D.D.L. Chung, G.C. Lee, Damage in carbon-reinforced concrete, monitored by electrical resistance measurement, Cement and Concrete Research 30 (5) (2000).